Electronic Supplementary Material (ESI) for RSC Advances.

Utilization of modified Dioscorea opposita Thunb as a novel biosorbent for the adsorption of indigo carmine in aqueous solutions

Yanzhuo Zhang[a]*, **Jun Li**[b]

[a]*School of Environment, Henan Normal University, Key Laboratory for Yellow River and Huai River Water Environmental and Pollution Control, Ministry of Education, Henan Key Laboratory for Environmental Pollution Control, Xinxiang, Henan 453007, P. R. China.*

[b]*The College of Architecture and Civil Engineering, The Key Laboratory of Beijing for Water Quality Science & Water Environment Recovery Engineering, Beijing University of Technology, Beijing 100124, Chin*a

Authors:

Yanzhuo Zhang. E-mail: 83995983@qq.com

Jun Li. E-mail: lijunbjut@163.com

*Corresponding author： Yanzhuo Zhang

E-mail: 83995983@qq.com.

Table S1 Element composition of DOT and DOT@PEI

Element	DOT		DOT@PEI	
	Weight percentage (%)	Atomic percentage (%)	Weight percentage (%)	Atomic percentage (%)
C	28.309	38.736	45.613	37.061
O	51.329	52.725	51.854	56.122
Mg	0.859	0.581	0.255	0.419
Si	1.000	0.585	0.346	0.657
P	0.902	0.479	0.178	0.374
S	1.294	0.663	0.089	0.193
Cl	0.905	0.419	0.142	0.341
K	8.051	3.384	0.448	1.186
Ca	3.585	1.470	0.635	1.721
Fe	0.265	0.078	0.026	0.099
Zn	3.502	0.880	0.413	1.827

Figure Captions

Fig. S1 SEM micrographs of (a) DOT and (b) DOT@PEI

Fig. S2 EDS spectra of (a) DOT and (b) DOT@PEI

Fig. S3 FTIR spectra of biosorbents: (a) DOT, (b) DOT@PEI

Fig. S4 BET isotherm of DOT@PEI

Fig. S5 The zeta potential of DOT and DOT@PEI (s) at varied pH conditions.

Fig. S6 Plots of (a) Langmuir isotherm model for the adsorption of Indigo Carmine onto the DOT@PEI at 20℃.

Fig. S7 Plots of (a) Freundlich isotherm models for the adsorption of Indigo Carmine onto the DOT@PEI at 20℃.

Fig. S8 Plots of (a) Temkin isotherm models for the adsorption of Indigo Carmine onto the DOT@PEI at 20℃.

Fig. S9 Pseudo-First-Order Kinetic Model for adsorption of Indigo Carmine onto the DOT@PEI at 20℃.

Fig. S10 Pseudo-Second-Order Kinetic Model for adsorption of Indigo Carmine onto the DOT@PEI at 20℃.

Fig. S11 Intraparticle diffusion model for adsorption of Indigo Carmine onto the DOT@PEI at 20℃.

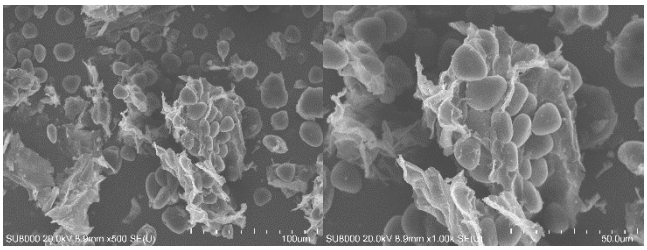

500×　　1000×

(a) DOT

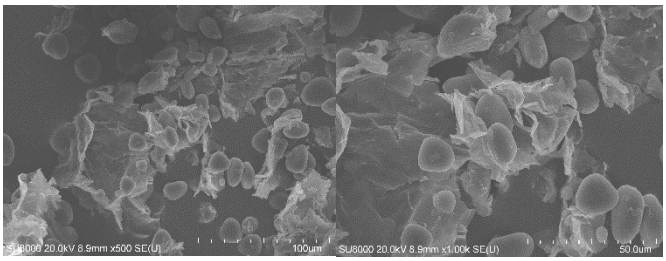

500×　　1000×

(b) DOT@PEI

Fig. S1 SEM micrographs of (a) DOT and (b) DOT@PEI

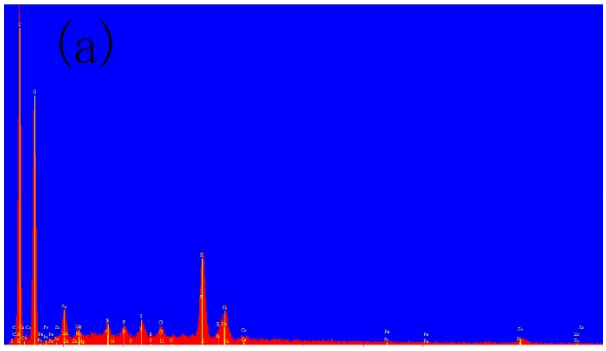

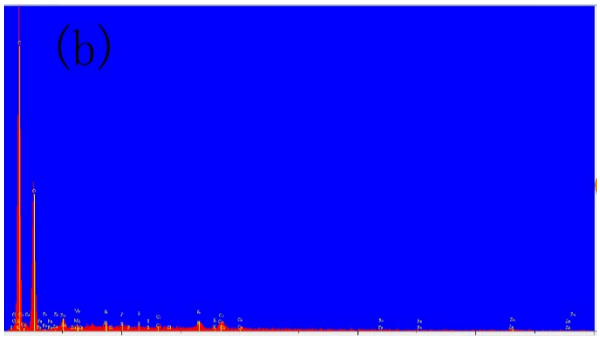

Fig. S2 EDS spectra of (a) DOT and (b) DOT@PEI

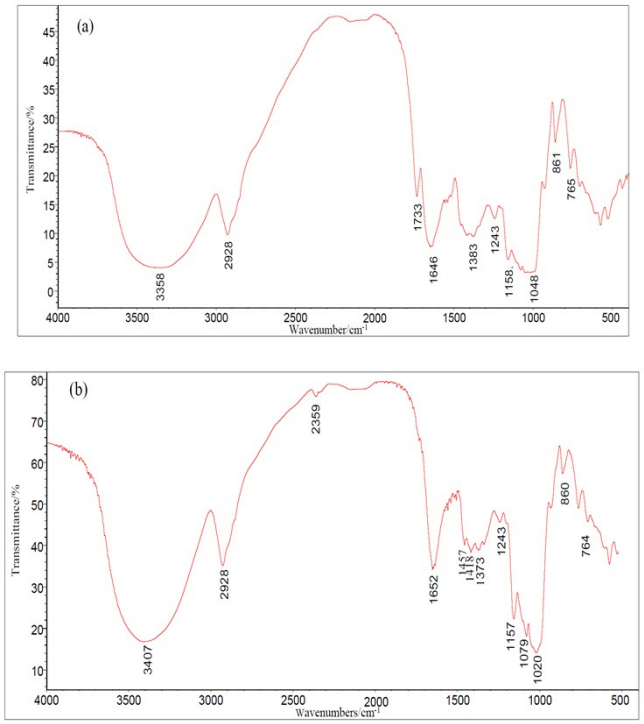

Fig. S3 FTIR spectra of biosorbents: (a) DOT, (b) DOT@PEI

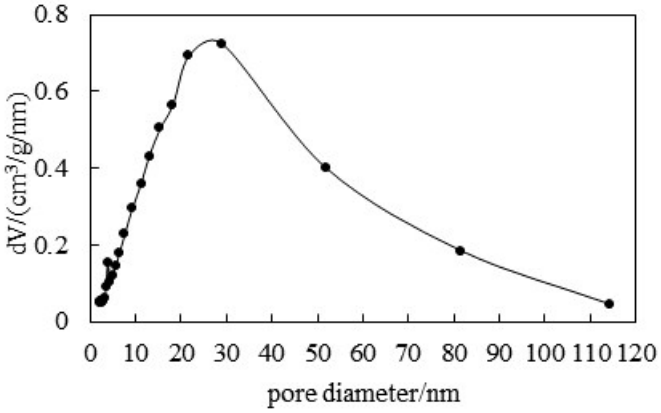

Fig. S4 BET isotherm of DOT@PEI

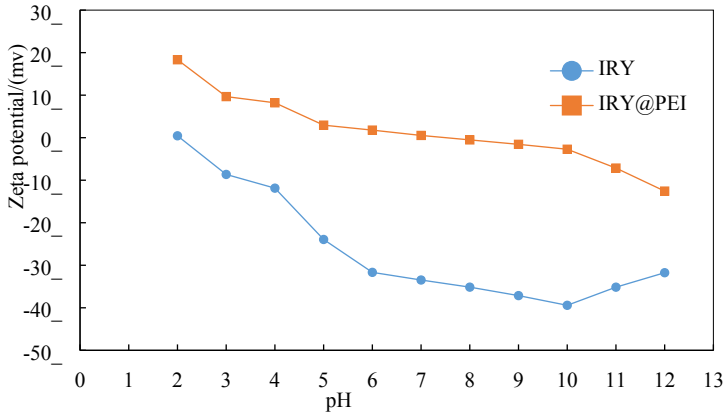

Fig. S5 The zeta potential of DOT and DOT@PEI (s) at varied pH conditions.

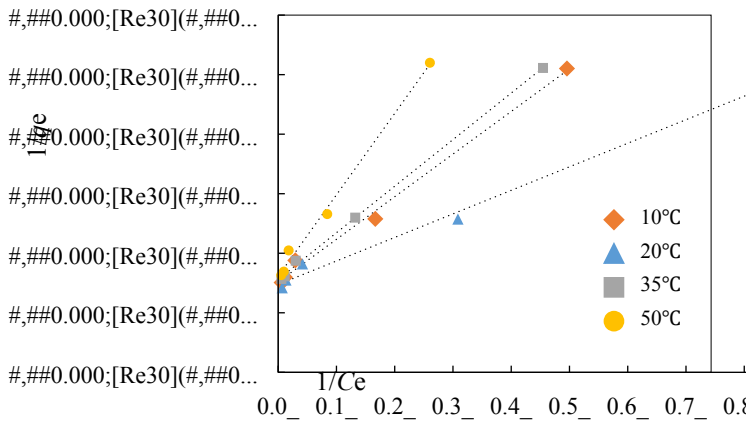

Fig. S6 Plots of (a) Langmuir isotherm model for the adsorption of Indigo Carmine onto the DOT@PEI at 20℃.

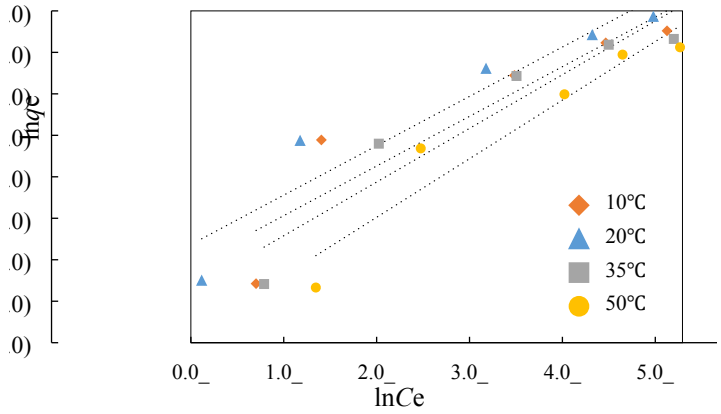

Fig. S7 Plots of (a) Freundlich isotherm models for the adsorption of Indigo Carmine onto the DOT@PEI at 20℃.

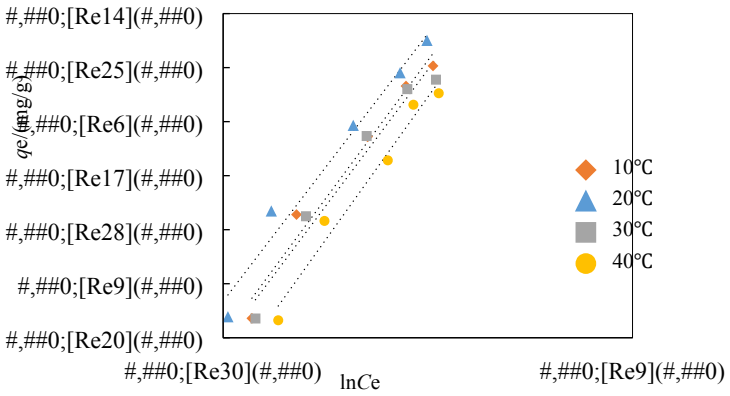

Fig. S8 Plots of (a) Temkin isotherm models for the adsorption of Indigo Carmine onto the DOT@PEI at 20℃.

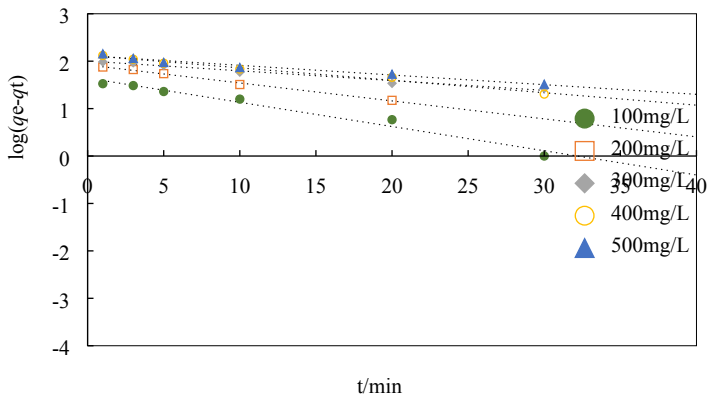

Fig. S9 Pseudo-First-Order Kinetic Model for adsorption of Indigo Carmine onto the DOT@PEI at 20℃.

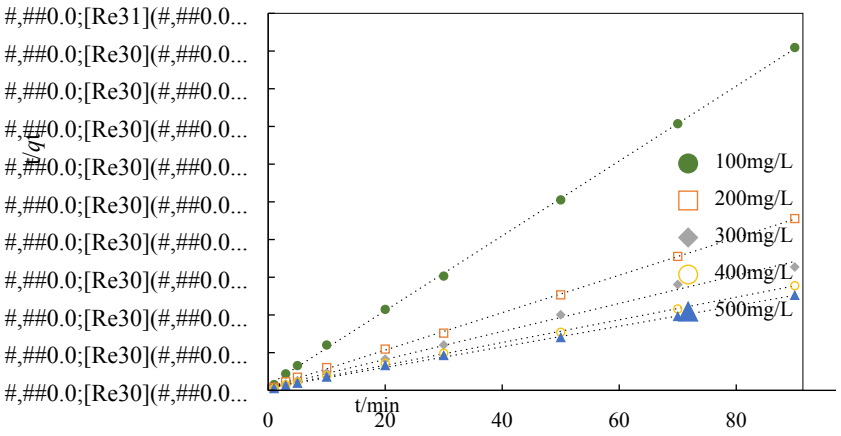

Fig. S10 Pseudo-Second-Order Kinetic Model for adsorption of Indigo Carmine onto the DOT@PEI at 20℃.

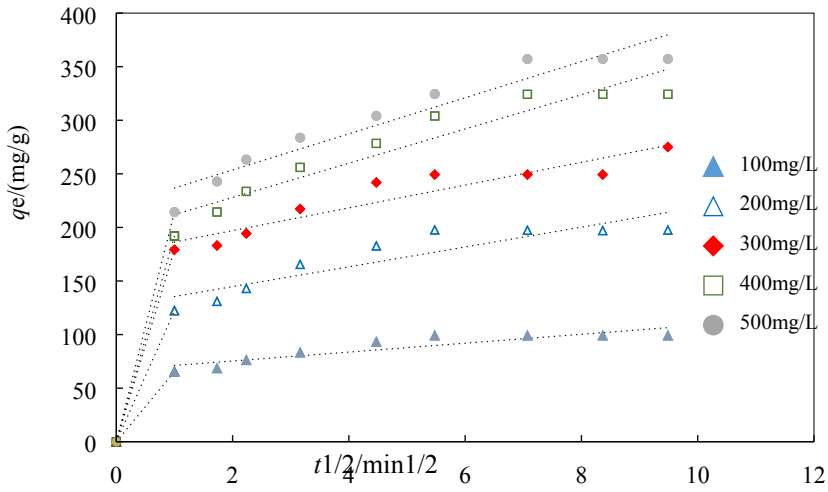

Fig. S11 Intraparticle diffusion model for adsorption of Indigo Carmine onto the DOT@PEI at 20℃.